

# Epidemic spreading on scale-free networks with correlations

北陸先端科学技術大学院大学 林 幸雄 (Yukio HAYASHI)  
Japan Advanced Institute of Science and Technology

**Abstract:** Many complex networks have a common structure called scale-free with power-law degree distributions, however the details such as the degree-degree correlations are different in social, technological, and biological systems. It has been shown that social networks tend to have positive correlations (assortative connections between nodes with similar degrees, such as hub-hub), however technological and biological networks tend to have negative correlations (disassortative connections between nodes with different degrees, such as low-high degrees). In this paper, we numerically investigate the epidemic spreading on the network with a variety of correlations: the assortative, uncorrelated, and disassortative mixings. In a simulation for the mean-field-like susceptible-infected-recovered model, we observe different epidemic behavior according to the types of correlations. Our results suggest that the assortative connections between nodes with similar degrees enhance the epidemic spreading more significantly than the uncorrelated and disassortative connections between cooperative nodes with high and low degrees.

## 1 Introduction

Self-organized complex networks have attracted a great attention to statistical physicists, computer scientists, and mathematical biologists, since many empirical studies have revealed the fact that a structure is commonly found in social, technological, and biological networks. The structure is called scale-free (SF) [2] and follows a power-law distribution  $P(k) \sim k^{-\gamma}$ ,  $2 < \gamma < 3$ , for the number of nodes with degree  $k$ . Since the heterogeneous characteristics of the SF network are crucial for the robustness of connectivity against failures [1], the efficiency of information delivery [3], and the spread of epidemic disease transmitted by means of social or sexual contacts, e-mails, Internet, and so forth [4], we expect that the evolutionary mechanisms and the structural properties of the SF network [1] are useful for maintaining and improving the efficiency and the robustness of power supply, communication, and economy systems.

On the other hand, recent studies classify networks according to types of connectivity correlations of nodes with their neighbors [5]; social networks tend to have assortative connections between peers with similar degrees [6][7], while technological or biological networks tend to have disassortative ones between those nodes with high degrees, namely hubs, and those with low degrees [5][8]. The properties for the epidemic incidence [9] and for the percolation [10] have been compared in the considered forms of correlations defined as a

weighted combination of the uncorrelated (or arbitrary correlated) term and the fully assortative term: a fully assortative connection allows only two nodes with the same degree to be connected. However the relation of the results stated above to the evolutionary mechanisms of network is still unclear. Only a few analytical forms of correlations have been derived from the tree model [11] and the configuration model [12]. Although the configuration model produces disassortative mixing (but not realises assortative one), a non-trivial distribution of degrees assumed in a factorizable form must be given for wiring in advance. Also, difficulties in estimating the conditional probability of degree-degree connectivity even from empirical data has been pointed out [13]. Apart from the evolutionary mechanisms, a numerical simulation has shown that the introduction of assortative hub-hub connections between different local areas on a lattice has the effects to shorten the average delivery time and to enlarge the spread of infection [14]. However, neither theoretical solutions nor numerical studies for the epidemic behavior have been reported except for the above forms of correlations.

We study epidemic spreading on the SF networks with a variety of assortative, disassortative, and uncorrelated connections, which are not specialized in social, technological, or biological systems. First, we review two growing network models: one is called the duplication-divergence model [15], which is equipped with a control parameter of connectivity correlations between the assortative and the disassortative mixings, and the other is called the directed growing model, in which the existence of correlations is suggested [13]. Then, we will estimate the conditional probability of degree-degree correlations from the average realizations of the growing network models. This estimation method can be applied to other network models. By using the estimated probability, we numerically investigate the epidemic behavior for the mean-field-like equations of the susceptible-infected-recovered/removed (SIR) model. We find different epidemic behavior according to the types of correlations.

## 2 Growing Network Models

Let us consider the growing network models shown in Figs. 1 (a) and (b). The following procedures are repeated until the network reaches to the required size  $N$ .

Dup: duplication-divergence model [15]

1. At each time step, a new node  $i'$  is added to the network.
2. Simultaneously, a node  $i$  is randomly chosen, and new (undirected) links between all the neighbors  $j$  of  $i$  and the new node  $i'$  are duplicated.
3. With probability  $q_v$ , a link between  $i$  and  $i'$  is established (self-interaction).
4. In the divergence process, each duplicated link is removed with probability  $1 - q_e$ .

These local rules are biologically plausible [16]. Note that larger  $q_v$  enhances the assortativity because the self-interaction means connecting a pair of nodes with similar degrees. In other words,  $q_v$  is a control parameter of the correlation.

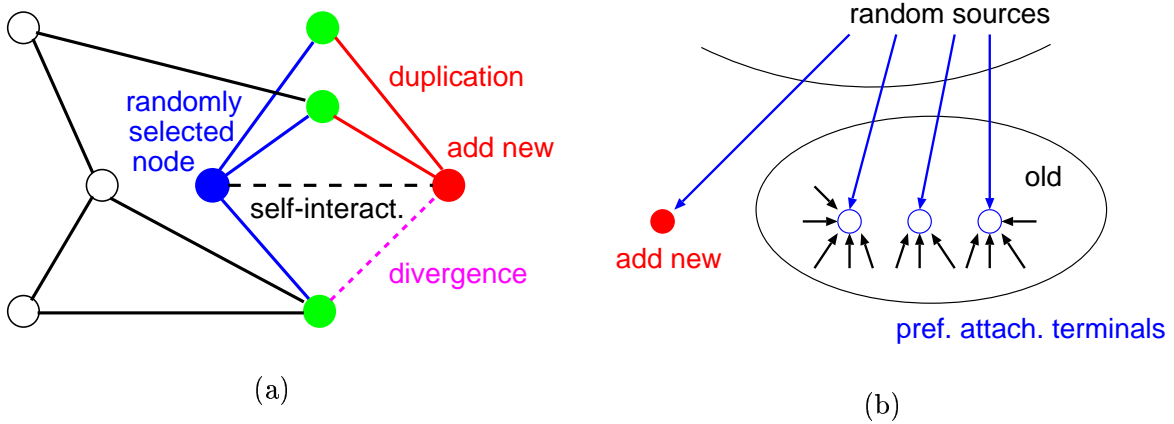


Fig 1: Growing network models. (a) In the duplication-divergence model, duplication links (red solid lines) between a new node (red circle) and all the neighbors (green circles) of a randomly chosen node (blue circle), and self-interaction (dashed line) are generated, but some links (magenta dashed line) are removed. (b) In the directed growing model, new links from randomly chosen sources to preferentially attached terminals emerge.

Dir: directed growing model [13]

1. At each time step, a new node is added and connected from a randomly chosen node.
2. Simultaneously,  $m'$  new links emerge from randomly chosen nodes in the network.
3. The terminals of the new links become attached to nodes chosen with shifted linear preference [11]: a node with in-degree  $k$  is chosen as the terminal of a new link with probability proportional to  $k + w$ , where  $w$  is a positive constant.

The generation of new links includes the wiring between old nodes at each time step. In addition, to keep the connectivity of network, the first procedure can be modified to the probabilistic addition of new nodes in Ref. [13]. If a multi-link between already connected nodes or self-loop is created, it is skipped in the directed growing model, while there is no such link in the duplication-divergence model. Note that directed models have a sense of reality: the sender and the receiver of transmitted information or objects are distinguished from each other on a directed link.

In the directed growing model, the rate equations [11] for the in-degree distribution are written as

$$\frac{dN_k}{d\tau} = \frac{m'}{m+w} [(k-1+w)N_{k-1} - (k+w)N_k] + \delta_{k,1}, \quad (1)$$

where  $m \stackrel{\text{def}}{=} m' + 1$ ,  $\gamma \stackrel{\text{def}}{=} 1 + (m+w)/m'$ ,  $w = m' \times (\gamma - 2) - 1$ , and  $\delta_{k,1}$  is Kronecker's delta,  $N_k$  denotes the number of nodes with degree  $k$  at time  $\tau$ . Then, we obtain the time-independent solution from  $n_k \sim N_k/\tau$ ,

$$n_k = \frac{(k-1+w)n_{k-1}}{k-1+w+1+(m+w)/m'} \sim k^{-\gamma}. \quad (2)$$

The second column of Table 1 shows the values of the parameters used in our simulation. Ass, Unc, and Dis denote the assortative, uncorrelated, and disassortative networks,

respectively. We regulate these values so that they produce similar average degrees  $\langle k \rangle$ , because it is obvious that the epidemic spreading becomes larger as the degrees increase. Fig. 2 shows distributions of the degree  $P(k) \stackrel{\text{def}}{=} N_k/N$  and the connectivity correlation  $\langle k_{nn} \rangle \stackrel{\text{def}}{=} \sum_l lP(l|k)$ , where  $P(l|k)$  is the conditional probability of the connections between nodes with degrees  $l$  and  $k$  in Dup, or the connections from nodes with in-degree  $l$  to those with  $k$  in Dir. The degree distributions exhibit the power-law behavior: the exponents are changed according to the values of parameter  $\gamma$  for Ass and Unc in Dir (Fig. 2 (b)), while they are close to each other in Dup (Fig. 2 (a)). The correlations are controlled between Ass and Dis in Dup (Fig. 2 (c)), while they are controlled between Ass and Unc that is nearly uncorrelated with very weak correlations in Dir (Fig. 2 (d)). If the connection links are replaced by reciprocal ones after the configuration of Dir, the degree distribution becomes exponential, and the correlation disappears.

Model		$q_v$	$q_e$	$\gamma$	$m'$	$\langle k \rangle$	$K_{min}$	$K_{max}$
Dup	Ass	0.9	0.42	-	-	7.463	45	122
	Unc	0.3	0.48	-	-	7.356	55	159
	Dis	0.1	0.5	-	-	7.395	62	237
Dir	Ass	-	-	3.0	7	7.33	80	142
	Unc	-	-	2.1	9	7.354	251	339

表 1: A set of parameters for the duplication-divergence and the directed growing models (denoted by Dup and Dir). Unnecessary parameters are marked by hyphens. The average degree of all nodes, the minimum and maximum degrees (in-degrees for directed links) of a hub node are measured over the 100 realizations of  $N = 10^3$ .

Next, we consider the SIR model in which individual nodes have three states: susceptible, infected, and recovered/removed. The densities of the nodes with degree (or in-degree in Dir)  $k$  in the respective states are denoted by  $s_k(t) = S_k(t)/N_k(t)$ ,  $\rho_k(t) = I_k(t)/N_k(t)$ ,  $r_k(t) = R_k(t)/N_k(t)$ . By definition, the normalization condition  $s_k(t) + \rho_k(t) + r_k(t) = 1$  holds at each time  $t$ . Here, we distinguish the time-scales  $\tau$  and  $t$  for evolution of network and spreading of viruses, respectively. After the construction of a network for the Dir or Dup model, the epidemics is propagated by contacts between infected and susceptible individuals (from infected nodes to susceptible nodes through directed links in Dir) at a rate denoted by  $b$ . The infected node is removed at a rate denoted by  $\delta$ . Once an individual gets infected and then recovers or removed, the state is never changed any more. The microscopic stochastic simulation needs very expensive computation for studying the epidemic properties, therefore a macroscopic mean-field approximation is useful. We consider the spreading on the averages of randomly generated networks for each of Dup and Dir.

Following Ref. [17], the mean-field-like rate equations for the evolution of densities can be expressed as

$$\frac{ds_k(t)}{dt} = -bks_k(t)\Theta_k(t), \quad (3)$$

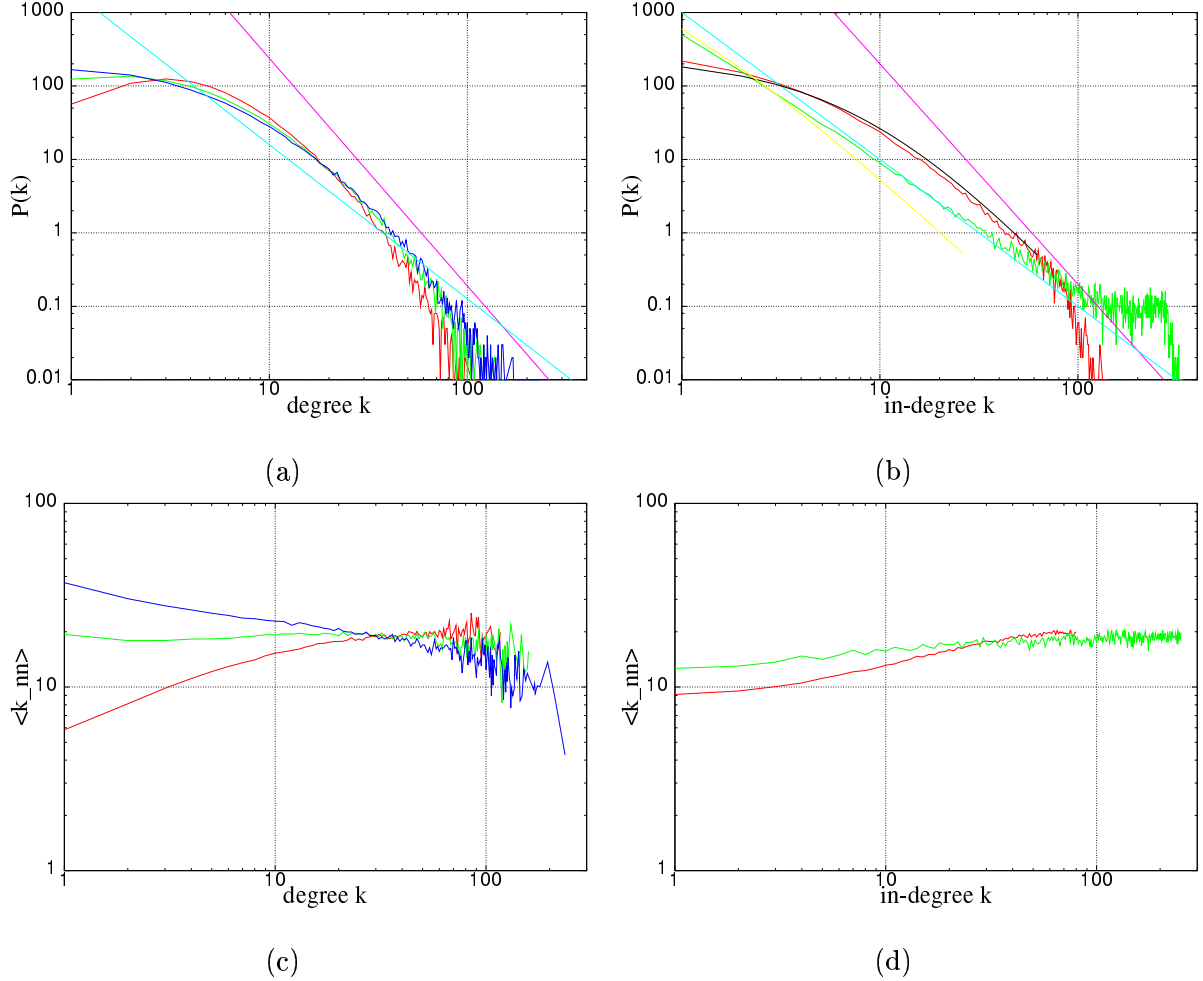


FIG 2: Distributions of degree and connectivity correlation. (a)  $P(k)$  for the degree in Dup, (b)  $P(k)$  for the in-degree in Dir, (c)  $\langle k_{nn} \rangle$  for the degree in Dup, (d)  $\langle k_{nn} \rangle$  for the in-degree in Dir. The guide lines show power-law behavior of exponents 2.1 (cyan) and 3.0 (magenta). In (b), the yellow and black lines for the analytical solutions of Eq (2) are well fitting the cases of  $\gamma = 2.1$  (green) and 3.0 (red). In (c) and (d), the red, green, and blue lines clearly show the correlations corresponding to the cases of Ass, Unc, and Dis in Table 1. The observations for very large degrees are statistically dropping and fluctuating. These are the averages over the 100 realizations.

$$\frac{d\rho_k(t)}{dt} = -\delta\rho_k(t) + bks_k(t)\Theta_k(t), \quad (4)$$

$$\frac{dr_k(t)}{dt} = \delta\rho_k(t),$$

where  $\Theta_k$  in the r.h.s of Eqs. (3) and (4) denotes the expectation of infection at degree  $k$ ,

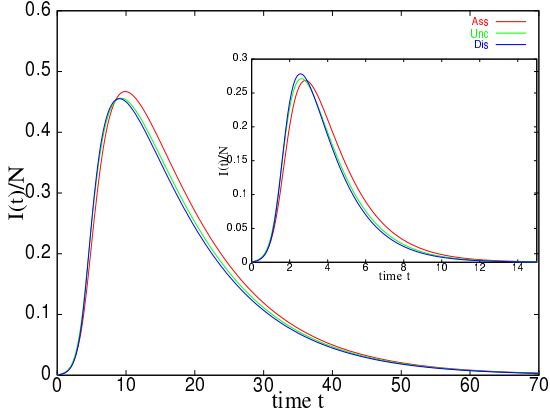
$$\Theta_k(t) \stackrel{\text{def}}{=} \begin{cases} \sum_{l=1}^{k_c} \frac{l-1}{l} P(l|k) \rho_l(t) & \text{for Dup,} \\ \sum_{l=1}^{k_c} P(l|k) \rho_l(t) & \text{for Dir,} \end{cases} \quad (5)$$

the factor  $(l-1)/l$  is added taking account of the fact that one of the links is not available for transmitting the infection because it was already used [17]. As applied to Fig. 2 (c) or (d), the  $P(l|k)$  is estimated from the average over 100 realizations for each parameter specification presented in Table 1. Since some degrees are missing in the range  $K_{min} < k < K_{max}$  over the realizations, we apply a cut-off value  $k_c$  defined by  $K_{min}$ .

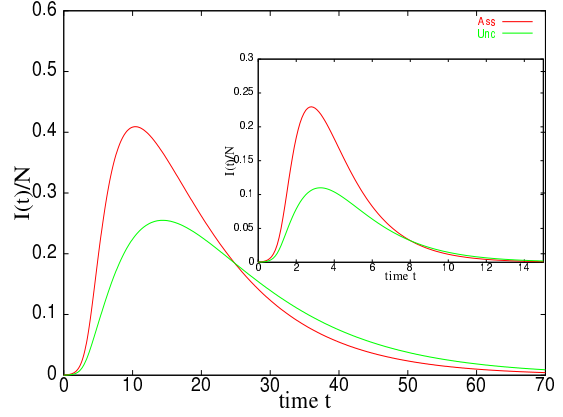
### 3 Simulation Results

We numerically investigate the dynamic behavior depends on the connectivity correlations by using the 4-th order Runge-Kutta method for Eqs. (3) and (4) with a step width  $\Delta t = 10^{-3}$ . In our simulation, we assume that an initial infection source is only on a hub with the degree  $k_c$ . Hence, for the other degrees  $k \neq k_c$  we set  $s_k(0) = 1$  and  $\rho_k(0) = r_k(0) = 0$ . This assumption is natural since the hub is much more vulnerable against infection through the active communications with the outside.

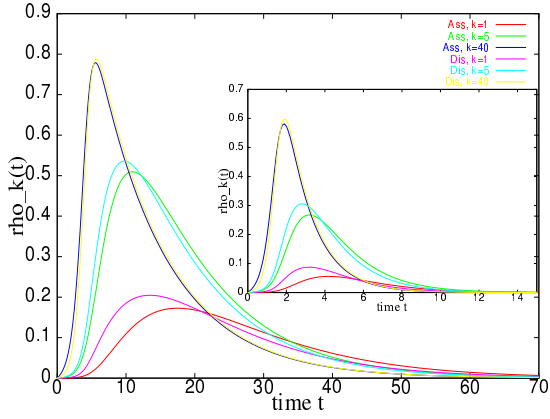
Figs. 3 (a) and (b) show the fraction of the infected nodes  $I(t)/N = \sum_k I_k/N$ . In the case of Ass (red line) it is slightly more insistent (Fig. 3 (a) for Dup) or larger (Fig. 3 (b) for Dir) than that in the case of Dis (blue line) and Unc (green line). The densities of the infected nodes  $\rho_k(t)$  in Figs. 3 (c) and (d) show a property similar to that of  $I(t)/N$ . The value of  $\rho_k(t)$  becomes larger as the degree  $k$  increases, therefore the infection from the nodes with high degrees are dominant in the  $\Theta_k$  of Eq. (5) in particular through assortative connections. Fig. 4 shows the epidemic incidence  $R(T) \stackrel{\text{def}}{=} \sum_k R_k(T)$ , which denotes the number of transitions from the total infected nodes. We set  $T = 100$  taking the convergent time in Fig. 3 into account. The incidence is higher in the assortative networks (red line) than that in uncorrelated (green line) or disassortative networks (blue line), except at  $b = 0.1$  and  $\delta = 0.7, 0.9$  in Dup. The exceptions suggest that the immune rate  $\delta$  is an important factor for small  $b$ . In other words, if we set  $\delta' = 1$  by a variable change of time  $t$  for Eqs. (3) and (4), we must use  $b' = b/\delta$ , which may be larger than 1, instead of  $0 < b < 1$ . The order of  $R(T)$  among Ass, Unc, and Dis is consistent with the results of stochastic simulation for the SIR model on the networks of Dup [19] (without substituting the estimated  $P(l|k)$  in the deterministic equations), although the peak value of  $\rho_k$  for Ass is smaller than that for Dis. These differences according to the types of correlations remarkably appear in Dir with smaller  $b$  as shown in Fig. 4 (b). Furthermore, similar results are also obtained in the directed growing model based on preferentially attached terminals and sources by the in- and out-degrees, respectively.



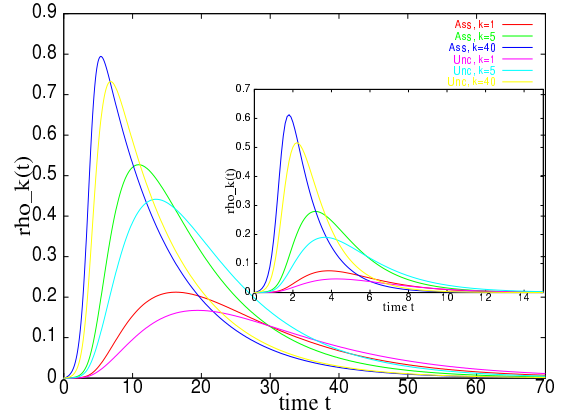
(a)



(b)



(c)



(d)

⊠ 3: Time evolutions of (a) the fraction of infected nodes  $I(t)/N$  in Dup, (b)  $I(t)/N$  in Dir, (c) each  $\rho_k(t)$  for  $k = 1, 5, 40$  in Dup, and (d)  $\rho_k(t)$  in Dir at  $b = 0.1$  and  $\delta = 0.1$ . Inset figures show similar behavior at  $b = 0.3$  and  $\delta = 0.5$  as some other example. Note that the value of  $I_k(t) = N_k \times \rho_k(t)$  is in the reverse order to  $k$  because of  $N_k \propto k^{-\gamma}$ .

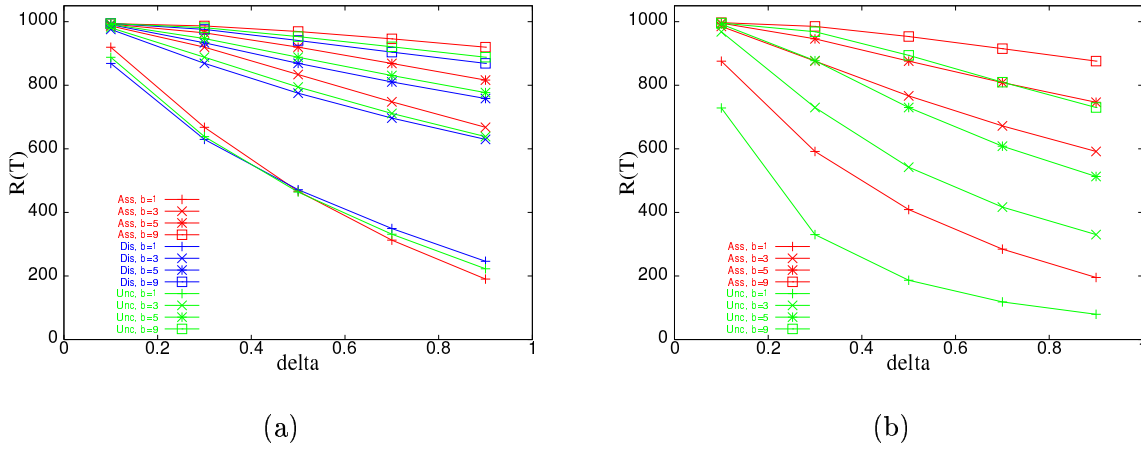


Fig 4: The epidemic incidence  $R(T)$  as a function of the immune rate  $\delta$  in (a) Dup, and (b) Dir. The red, green, and blue lines correspond to the cases of Ass, Unc, and Dis at  $b = 0.1, 0.3, 0.5, 0.7$  marked by the plus, cross, asterisk, and open square, respectively.

## 4 Conclusion

In summary, we have numerically found different spreading properties on SF networks according to the connectivity correlations estimated from the averages of the growing models [13][15]. The differences are remarkable in the directed model. The results suggest that assortative connections enhance the epidemic spreading, and also they could contribute to improve the efficiency of information delivery. In contrast, the disconnections or setting gatekeepers between nodes with similar degrees becomes a local defense strategy such as acquaintance immunization [18] for the spreading of viruses. However, the differences are small, and may depend on network models and/or on some parameters (e.g. infection and immune rates). Further works will be carefully considered for comprehending the effects of correlations on the spreading.

## 参考文献

- [1] R. Albert, H. Jeong, and A.-L. Barabási, *Nature* **406**, 378, (2000).
- [2] A.-L. Barabási, R. Albert, and H. Jeong, *Physica A* **272**, 173, (1999).
- [3] R.F.i Cancho, and R.V. Solé, *SantaFe Inst. Working Paper*, 01-11-068, (2001).
- [4] R. Pastor-Satorras, and A. Vespignani, *Evolution and Structure of the Internet, -A Statistical Physics Approach-*, Cambridge, 2004.
- [5] A. Vázquez, R. Pastor-Satorras, and A. Vespignani, *Phys. Rev. E* **65**, 066130, (2002).
- [6] A. Capocci, G. Caldarelli, and P. De Los Rios, *Phys. Rev. E* **68**, 047101, (2003).
- [7] M.E.J. Newman, *Phys. Rev. Lett.* **89**, 208701, (2002).



- [8] M.E.J. Newman, *Phys. Rev. E* **67**, 026126, (2003).
- [9] Y. Moreno, J.B. Gómez, and A. F. Pacheco, *Phys. Rev. E* **68**, 035103(R), (2003).
- [10] A. Vázquez, and Y. Moreno, *Phys. Rev. E* **67**, 015101(R), (2003).
- [11] P.L. Krapivsky, and S. Redner, *Phys. Rev. E*, **63**, 066123, (2001).
- [12] J. Park, and M.E.J. Newman, *Phys. Rev. E* **68**, 026112, (2003).
- [13] S.N. Dorogovtsev, and J.F.F. Mendes, *Evolution of Networks -From Biological Nets to the Internet and WWW*, Oxford University Press, 2003.
- [14] B.K. Singh, and N. Gupte, e-print *cond-mat/0312090*.
- [15] A. Vázquez, *Phys. Rev. E* **67**, 056104, (2003).
- [16] R.V. Solé, R. Pastor-Satorras, E. Smith, and T. Kepler, *Adv. Complex Syst*, **5**, 43, (2002). In S. Bornholdt, and H.G. Schuster (eds.) *Handbook of Graphs and Networks -From the Genome to the Internet-*, Chapter 7, pp.145-167, WILEY-VCH, 2003.
- [17] M. Boguñá, and R. Pastor-Satorras, e-print *cond-mat/0301149*, In R. Pastor-Satorras et. al (eds.) *Lecture Notes in Physics 625*, Chapter 7, pp.127-147, Springer, 2003.
- [18] R. Cohen, S. Havlin, and D. ben-Avraham, *Phys. Rev. Lett.* **91**, 247901, (2003).
- [19] S. Tanno, and Y. Hayashi, *Proc. of the 2005 Symposium on Network Ecology*, pp85.-92, in Japanese (2005).